ACS Pharmacology & Translational Science

pubs.acs.org/ptsci

Letter

Preclinical Development of the Na-K-2Cl Co-transporter-1 (NKCC1) Inhibitor ARN23746 for the Treatment of Neurodevelopmental Disorders

Annalisa Savardi,* Andrea Patricelli Malizia, Marco De Vivo, Laura Cancedda, and Marco Borgogno*

Cite This: *ACS Pharmacol. Transl. Sci.* 2023, 6, 1−11

Read Online

ACCESS | Metrics & More | Article Recommendations | Supporting Information

ABSTRACT: Alterations in the expression of the Cl^- importer Na-K-2Cl co-transporter-1 (NKCC1) and the exporter K-Cl co-transporter 2 (KCC2) lead to impaired intracellular chloride concentration in neurons and imbalanced excitation/inhibition in the brain. These alterations have been observed in several neurological disorders (e.g., Down syndrome and autism). Recently, we have reported the discovery of the selective NKCC1 inhibitor "compound ARN23746" for the treatment of Down syndrome and autism in mouse models. Here, we report on an extensive preclinical characterization of ARN23746 toward its development as a clinical candidate. ARN23746 shows an overall excellent metabolism profile and good brain penetration. Moreover, ARN23746 is effective in rescuing cognitive impairment in Down syndrome mice upon *per os* administration, in line with oral treatment of neurodevelopmental disorders. Notably, ARN23746 does not present signs of toxicity or diuresis even if administered up to 50 times the effective dose. These results further support ARN23746 as a solid candidate for clinical trial-enabling studies.

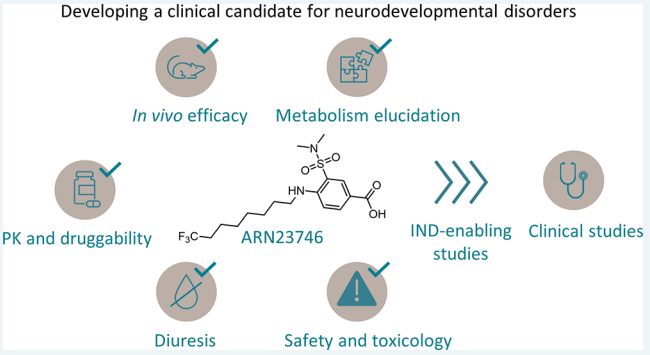

KEYWORDS: *NKCC1, Down syndrome, autism, drug development, neurological disorders*

Over the past 20 years, several lines of evidence have indicated that intervening on the levels of intracellular chloride concentration $[Cl^-]_i$ represents a promising approach for treating different neurological disorders, including Down syndrome (DS).[1−3] $[Cl^-]_i$ in neurons is mainly regulated by the electroneutral chloride co-transporters NKCC1 and KCC2. In agreement with altered Cl^- homeostasis, brain samples from both a mouse model of DS (the Ts65Dn mouse) and human subjects with DS show an increased NKCC1 expression, leading to an altered NKCC1/KCC2 expression ratio. Alterations in the NKCC1/KCC2 expression ratio (due to either higher expression of NKCC1 and/or lower expression of KCC2) have been also reported in a number of brain disorders, both in animal models and in human samples.[1,2,4] These co-transporter alterations lead to a pathological depolarizing (vs physiological hyperpolarizing and inhibitory) γ-aminobutyric acid (GABA) neurotransmitter action through Cl^--permeable $GABA_A$ receptors in mature neurons. In this context, we have recently presented the discovery and characterization of a new class of selective NKCC1 inhibitors able to restore physiological $[Cl^-]_i$ in DS neurons grown in culture. In particular, the lead compound of this new class (ARN23746) showed high potency and selectivity toward NKCC1 *in vitro*.[5] Most notably, ARN23746 demonstrated efficacy in restoring core symptoms in mouse models of DS and autism upon intraperitoneal (IP) administration *in vivo*, thus providing a possible new therapeutic approach for DS and autism.[5]

In this work, we further assessed some drug-likeness properties, the metabolic profile, the efficacy upon oral administration, and the toxicology of ARN23746. Our new data provide additional information supporting ARN23746 as a solid drug candidate for advanced development toward a viable treatment option for DS, autism spectrum disorder, and possibly other brain conditions that present altered NKCC1/KCC2 expression ratio.

First, to better characterize the *in vitro* potency of our lead candidate ARN23746 in inhibiting NKCC1, we performed two dose−response curve studies under diverse experimental conditions, as already described in our previous works.[5,6] Initially, we took advantage of the Cl^--influx assay performed in human HEK293T (human embryonic kidney 293) cells

Received: October 6, 2022
Published: January 4, 2023

ACS Publications

© 2023 American Chemical Society

https://doi.org/10.1021/acsptsci.2c00197
ACS Pharmacol. Transl. Sci. 2023, 6, 1−11

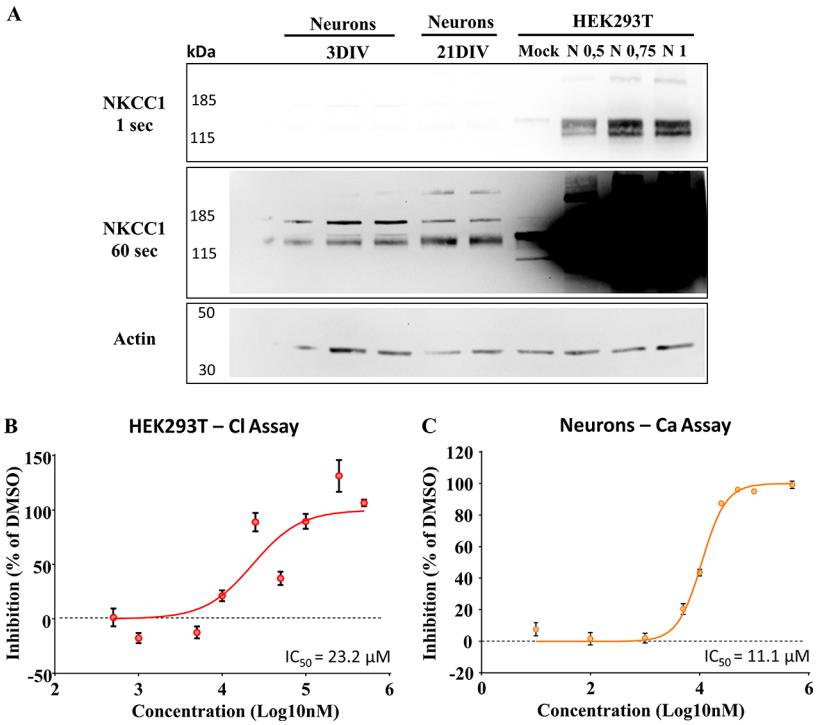

Figure 1. *In vitro* characterization of ARN23746. (A) Representative immunoblots showing the highly different expression of NKCC1 in the different cells used for the *in vitro* assay. From the left, 3DIV neurons, 21DIV neurons, and HEK293T cells non-transfected (Mock) or over-expressing different amounts of NKCC1 plasmid (0.5, 0.75, and 1 μg). To appreciate the different NKCC1 expression (signal), membranes were exposed at two different time points (1 s, 60 s). On the left kilodaltons (kDa) of the marker bands are indicated. (B) Dose−response curve of ARN23746 in HEK293T cells over-expressing NKCC1 with Cl^--influx assay. Quantification of the mean ± SEM of NKCC1 inhibition by ARN23746 at the indicated concentrations (n = 3−10 for each concentration; one outlier was excluded from concentrations 50 μM and 500 μM based on Grubbs's test). Non-linear fit of log(inhibitor) vs normalized response-variable slope (degrees of freedom = 152, R^2 = 0.56). (C) Dose−response curve of ARN23746 in young neurons with Ca^{2+}-influx assay. Quantification of the mean ± SEM of Ca^{2+}-influx inhibition by ARN23746 at the indicated concentrations (n = 4−10 for each concentration; one outlier was excluded from concentrations 1 μM and 10 μM; two outliers were excluded from concentrations 5 μM and 100 μM based on Grubbs's test). Non-linear fit of log(inhibitor) vs normalized response-variable slope (degrees of freedom = 168, R^2 = 0.94).

transfected with NKCC1 (or the corresponding empty plasmid as control-mock) together with the Cl^--sensitive, membrane-tagged yellow fluorescent protein (mbYFPQS) plasmid. Notably, these experimental conditions lead to very high levels of NKCC1 over-expression (Figure 1A and Figure S1), compared to physiological levels of neurons at diverse stages of maturation. This represents a very stringent condition that we specifically implemented to have an assay that could be used for wide and efficient first screenings. In this way, we could identify and select new hit compounds capable of inhibiting NKCC1 even when highly over-expressed. Since mbYFPQS fluorescence is inversely dependent on $[Cl^-]_i$, we monitored the decrease in fluorescence upon application of NaCl (74 mM) and the consequent Cl^- influx via NKCC1 in the transfected cells kept in a Cl^--free hypotonic assay solution. By fitting the dataset on NKCC1 inhibition by ARN23746 at different concentrations (0.05−500 μM range), expressed on a logarithmic scale with a non-linear curve, we extrapolated an IC_{50} corresponding to 23.2 μM (Log IC_{50} = 4.36 ± 0.06, Figure 1B).

Next, we performed a study in cells physiologically expressing NKCC1 (vs the over-expression system in HEK293 cells, as reported in Figure 1A and Figure S1). In particular, we assessed the potency of ARN23746 in reducing the depolarizing strength of $GABA_A$ergic transmission in immature neurons. Indeed, immature neurons during development express high levels of NKCC1, leading to high $[Cl^-]_i$ and depolarizing GABA action.[7] We performed a dose−response curve study in immature neurons taking advantage of a calcium (Ca^{2+})-influx assay, as already described in our previous works.[5,6] Briefly, this assay is based on the endogenous high NKCC1/KCC2 expression ratio in immature neurons, which causes depolarizing actions of GABA able to activate voltage-gated Ca^{2+} channels, thus leading to a Ca^{2+} increase in neurons. NKCC1 inhibitors significantly inhibit Ca^{2+} influx upon GABA application in immature neurons, as previously demonstrated.[5] We thus used a fluorescent Ca^{2+}-sensitive dye (Fluo4) to monitor intracellular Ca^{2+} variations, as an indirect measure of variation in GABAergic transmission, upon application of GABA (100 μM) in the presence of ARN23746. This assay can be considered a proxy (although indirect measurement) of GABA signaling efficacy in a physiological condition in neurons. By fitting the dataset on inhibition of Ca^{2+} responses by ARN23746 at different concentrations (0.01−500 μM range), expressed on a logarithmic scale with a non-linear curve, we extrapolated an IC_{50} corresponding to 11.1 μM (Log IC_{50} = 4.05 ± 0.01, Figure 1C). Notably, in a previous experiment assessing the direct activity of ARN23746 on modulation of $[Cl^-]_i$ in neurons through the Cl^--sensor MQAE (*N*-(ethoxycarbonylmethyl)-6-methoxyquinolinium bromide), we found that 10 μM of ARN23746 was able to completely restore the physiological $[Cl^-]_i$ in DS neurons to the level of wild-type,[5] suggesting an IC_{50} < 10 μM. This indicates that, depending on

https://doi.org/10.1021/acsptsci.2c00197
ACS Pharmacol. Transl. Sci. 2023, 6, 1−11

A

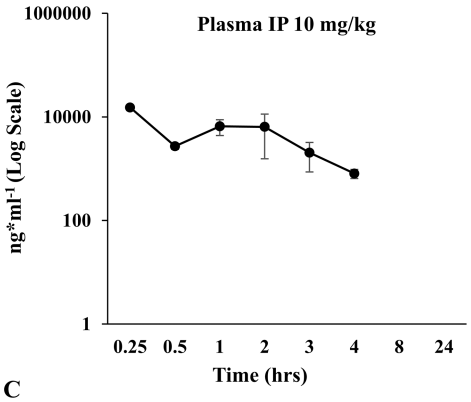

B

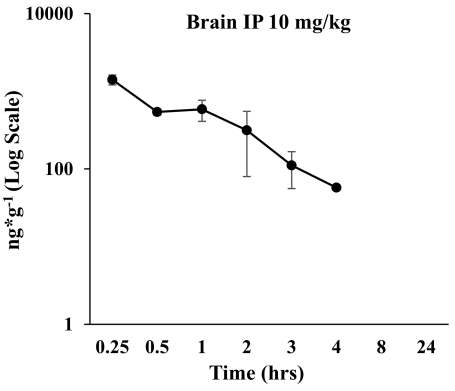

C

IP PK Parameters (10 mg/kg)							
	C_{MAX} (ng/g or ng/mL)	C_{MAX} (nM)	Tmax (hr)	T1/2 (hr)	AUC_{last} (h*ng/mL or ng/g)	AUC_{last} (h*nM)	Mean brain/plasma ratio
Brain	1410	3435	0.25	0.87	1450	3534	0.093
Plasma	15200	37033	0.25	0.93	18629	45387	

D

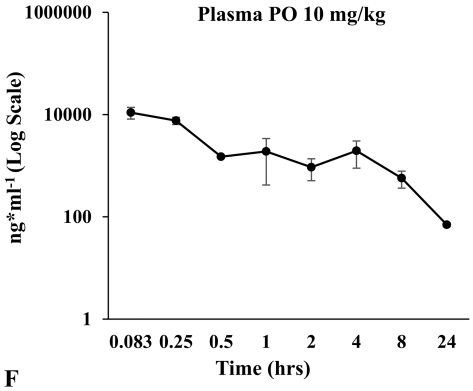

E

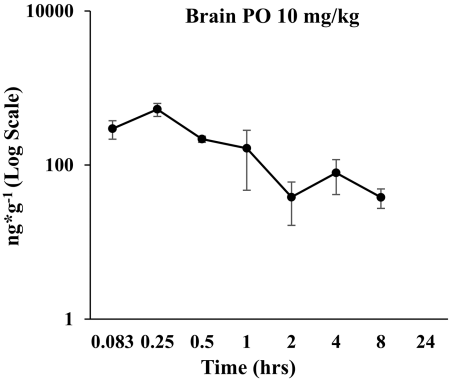

F

PO PK Parameters (10 mg/kg)							
	C_{MAX} (ng/g or ng/mL)	C_{MAX} (nM)	Tmax (hr)	T1/2 (hr)	AUC_{last} (h*ng/mL or ng/g)	AUC last (h*nM)	Mean brain/plasma ratio
Brain	529	92.9	0.25	3.7	724	1765	0.068
Plasma	10973	171	0.08	4.4	18533	45153	

Figure 2. *In vivo* pharmacokinetic profile of ARN23746. (A) Mouse brain PK profile of ARN23746 following IP administration at 10 mg/kg. (B) Mouse plasmatic PK profile of ARN23746 following IP administration at 10 mg/kg. (C) Observed and calculated PK parameters of ARN23746 after IP administration. (D) Mouse plasmatic PK profile of ARN23746 following PO administration at 10 mg/kg. (E) Mouse brain PK profile of ARN23746 following PO administration at 10 mg/kg. (F) Observed and calculated PK parameters of ARN23746 after PO administration. Data represent mean ± SEM from 3 independent experiments.

the type of measurement (direct vs indirect quantification of the effect of the compound) and on the *in vitro* system used (HEK vs neurons, NKCC1 over-expression vs physiological expression during development; Cl^--sensitive dyes and sensors vs Ca^{2+} sensors), the values of IC_{50} may vary substantially. In our experiments, ARN23746 showed the best potency in the cellular assay directly measuring $[Cl^-]_i$ in neurons (MQAE Cl imaging, IC_{50} < 10 μM).[5]

Then, we proceeded with *in vitro* characterizations of the permeability and metabolic stability of ARN23746. Several *in vitro* systems can be used to determine passive permeability, which is crucial to predict whether a molecule has the potential to cross the blood−brain barrier (BBB) *in vivo*.[8] Typically, the lipophilicity of the molecule is the main driver of permeability. However, multiple efflux mechanisms throughout the BBB (e.g., the P-glycoprotein (P-gp) and the Breast Cancer Resistance Protein (BCRP)) may contribute to low brain exposure. Several methods can be used to determine the contribution of these transporters on the permeability of CNS-targeted compounds *in vitro*. This further helps in the identification of lead compounds for neuroscience drug discovery. For these reasons, we determined passive perme-

https://doi.org/10.1021/acsptsci.2c00197
ACS Pharmacol. Transl. Sci. 2023, 6, 1−11

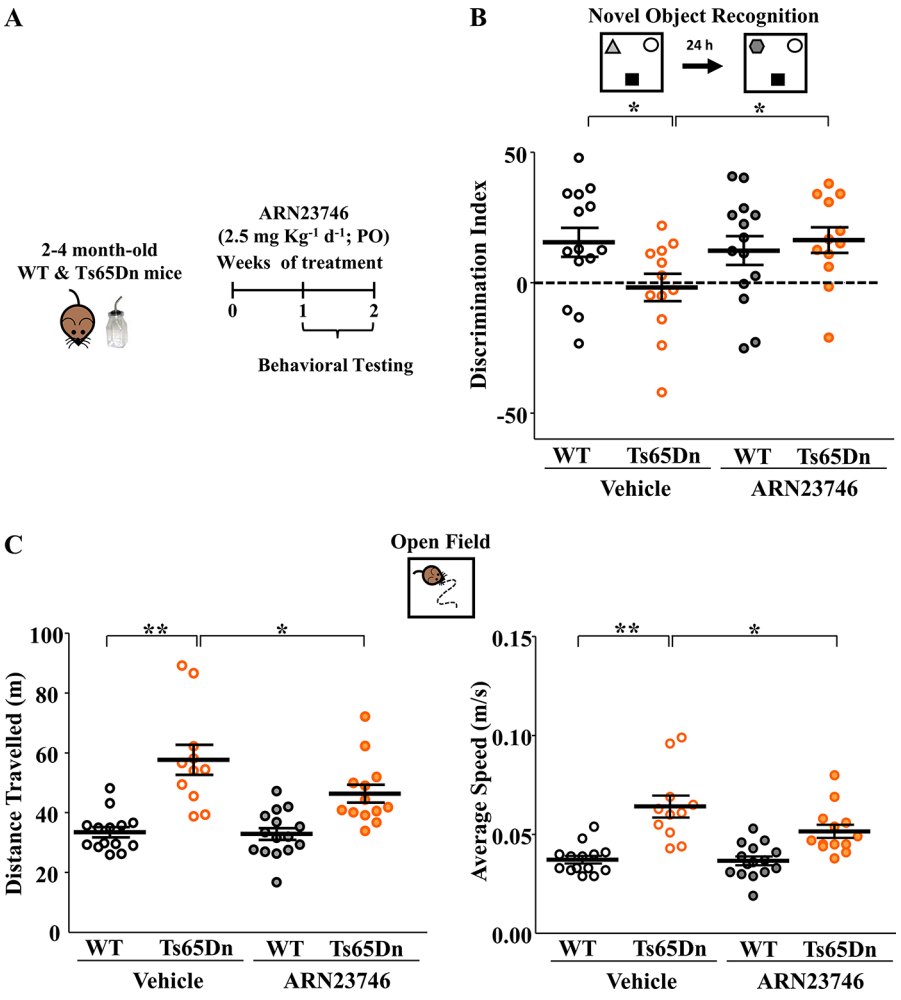

Figure 3. ARN23746 rescues cognitive impairment and hyperactivity in the Ts65Dn mouse model of Down syndrome upon oral administration. (A) Schematic cartoon of the experimental protocol for the treatment of adult WT and Ts65Dn mice with ARN23746 for *in vivo* efficacy assessment of improved cognitive impairment and hyperactivity in DS mice. (B) Top, schematic representation of the novel-object recognition task. Bottom, quantification of the mean ± SEM and single animal cases of the discrimination index in mice treated with the indicated drugs (no. of single animals: WT Vehicle = 14, Ts65Dn Vehicle = 12, WT ARN23746 = 14, Ts65Dn ARN23746 = 12; two-way ANOVA on ranks, $F_{\text{interaction (1,48)}} = 4.155$, $P = 0.047$, Tukey's *post hoc* test, $^{*}P < 0.05$). (C) Top, schematic representation of the open-field test. Bottom left, quantification of the mean ± SEM and single animal cases of the distance traveled during the test in mice treated with the indicated drugs (no. of single animals: WT Vehicle = 14, Ts65Dn Vehicle = 11, WT ARN23746 = 15, Ts65Dn ARN23746 = 13; two-way ANOVA, $F_{\text{genotype (1,50)}} = 8.666$, $P = 0.005$, Tukey's *post hoc* test, $^{*}P < 0.05$, $^{**}P < 0.01$). Bottom right, quantification of the mean ± SEM and single animal cases of the average walking speed in mice treated with the indicated drugs (no. of single animals: WT Vehicle = 14, Ts65Dn Vehicle = 11, WT ARN23746 = 15, Ts65Dn ARN23746 = 13; two-way ANOVA, $F_{\text{genotype (1,50)}} = 8.647$, $P = 0.005$, Tukey's *post hoc* test, $^{*}P < 0.05$, $^{**}P < 0.01$). One outlier was excluded from the Ts65Dn Vehicle group in the open-field test based on Grubbs's test.

ability in Madin−Darby Canine Kidney-Multi-Drug resistance 1 (MDCKII-MDR1) cells heterologously expressing human P-gp. The assay is based on the bi-directional transport of the test compound, and it also allows the calculation of the passive permeability, when tested in the presence of a known P-gp inhibitor. Importantly, ARN23746 showed a high passive permeability of 150 nm·s^{-1} and an efflux ratio of 1.3 (Table S1A), both in the presence and not of the P-gp inhibitor verapamil. This indicated that ARN23746 is not a P-gp substrate. Furthermore, we observed no BCRP interaction when we tested ARN23746 in polarized Caco-2 cells (Table S1A). Altogether, ARN23746 showed good permeability and good potential to efficiently cross the BBB, without interacting with efflux transporters. We thus integrated these *in vitro* data with *in vivo* pharmacokinetic studies to better quantify its brain penetration ability (*vide infra*).

We also performed a preliminary evaluation of ARN23746 metabolism in hepatocytes from different species, considering future toxicology studies. Consistent with microsomal stability data (>60 min in mouse, Table S1B), ARN23746 showed an extended half-life in both rodent and human hepatocytes (Table S1B). Moreover, metabolites identification (MetID) experiments conducted in rodent hepatocytes revealed that the compound is metabolized mainly through oxidative pathways in both rat and mouse (Table S1C). In these species, N-demethylation of the sulfonamide and oxidation of the long alkyl chain in position 3 was predominant. Nevertheless, conjugation metabolism, particularly O-glucuronidation, was also observed in rodent hepatocytes, although to a lower extent compared to dealkylation and oxidation (Table S1C). Interestingly, the main metabolic pathway in human hepatocytes was O-glucuronidation (Table S1C), and the overall half-life and intrinsic clearance were similar to those

https://doi.org/10.1021/acsptsci.2c00197
ACS Pharmacol. Transl. Sci. 2023, 6, 1−11

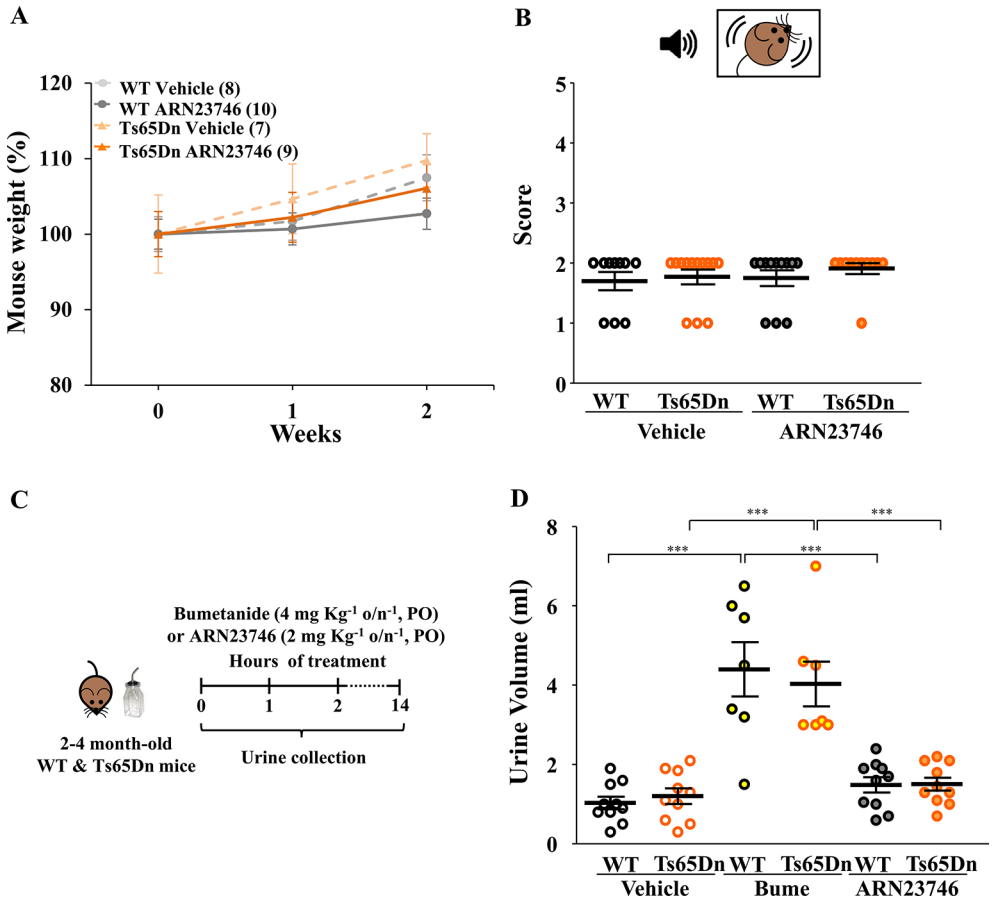

Figure 4. ARN23746 does not show an overt toxic effect after 2 weeks of sub-chronic PO treatment in mice. (A) Quantification of the body weight of WT and TS65Dn mice across the 2 weeks of treatment with vehicle (control) or ARN23746. Chronic treatment with ARN23746 does not affect body weight either in WT or in Ts65Dn mice (no. of single animals: WT Vehicle = 8, Ts65Dn Vehicle = 7, WT ARN23746 = 10, Ts65Dn ARN23746 = 9). (B) Top, schematic representation of the acoustic startle reactivity response test. Bottom, mean ± SEM and single animal cases of the average score of acoustic startle reactivity response reflex in adult mice treated sub-chronically with indicated drugs. The score scale indicates 0 = no response, 1 = mild response, and 2 = complete response to the acoustic stimulus (no. of single animals: WT Vehicle = 10, Ts65Dn Vehicle = 13, WT ARN23746 = 12, Ts65Dn ARN23746 = 11). (C) Schematic cartoon of the experimental protocol for the treatment of adult WT and Ts65Dn mice to assess the diuretic effect. (D) Quantification of the mean ± SEM and single animal cases of the urine volume collected for 14 h overnight in mice treated orally with the indicated drugs (no. of single animals: WT Vehicle = 10, Ts65Dn Vehicle = 10, WT Bume = 7, Ts65Dn Bume = 7, WT ARN23746 = 10, Ts65Dn ARN23746 = 10; two-way ANOVA on ranks, $F_{\text{treatment }(2,48)} = 31.335$, $P < 0.001$, Tukey's *post hoc* test, ***$P < 0.001$).

observed in rodent hepatocytes. However, the comparison between the levels of O-glucuronidation in rat hepatocytes and human hepatocytes indicated that the rate of formation of the O-glucuronide in rat was sufficient to recapitulate human metabolism in toxicology studies (Table S1C). Nevertheless, further studies in dog and non-human primates (NHP) hepatocytes are needed to cover metabolism identification and toxicology in non-rodent species to fulfill all the regulatory safety requirements.

Since ARN23746 showed an optimal *in vitro* profile, we proceeded with further *in vivo* characterization. First, we studied the pharmacokinetic (PK) profile by two different routes of administration of ARN23746 in mouse: (i) IP injection at 10 mg/kg ($n = 3$ mice for each time point) and (ii) *per os* (PO) treatment at 10 mg/kg ($n = 3$ mice for each time point). During these PK studies, via either IP or PO administration, ARN23746 did not cause any clinical sign or tolerability issue in the treated animals. That is, we observed no treatment-related adverse clinical signs. The peak plasma concentration for IP was observed at 15 min after administration, and the concentration of ARN23746 reached a C_{max} of 15 200 ng/mL (Figure 2A, C). Interestingly, we observed a rebound in the plasmatic concentration of the compound between the 30 min and 60 min time points (Figure 2A). Possibly, this rise in plasmatic concentration was due to enterohepatic cycling of the compound due to the presence of the O-glucuronide, which can be metabolized back in the intestine to the free drug.[9] Moreover, the enhancement of plasmatic concentration between 30 min and 60 min also led to an increase in the brain concentration between these two time points following IP administration (Figure 2B). As a result, brain levels of ANR23746 following IP administration were in line with the plasmatic exposure levels of the compound. The highest concentration was observed at T_{max} = 15 min after administration, resulting in a C_{max} of 1410 ng/g and corresponding to a brain−plasma ratio of 0.093 (Figure 2C). The PO profile of ARN23746 presented a rapid distribution, with a C_{max} of 10 937 ng/mL at 5 min after administration, followed by a slower exposure phase (Figure 2D, F). The compound was still measurable in plasma after 8 h at a 573 ng/mL concentration, resulting in an overall similar plasmatic exposure when compared to IP administration (AUC

https://doi.org/10.1021/acsptsci.2c00197
ACS Pharmacol. Transl. Sci. 2023, 6, 1−11

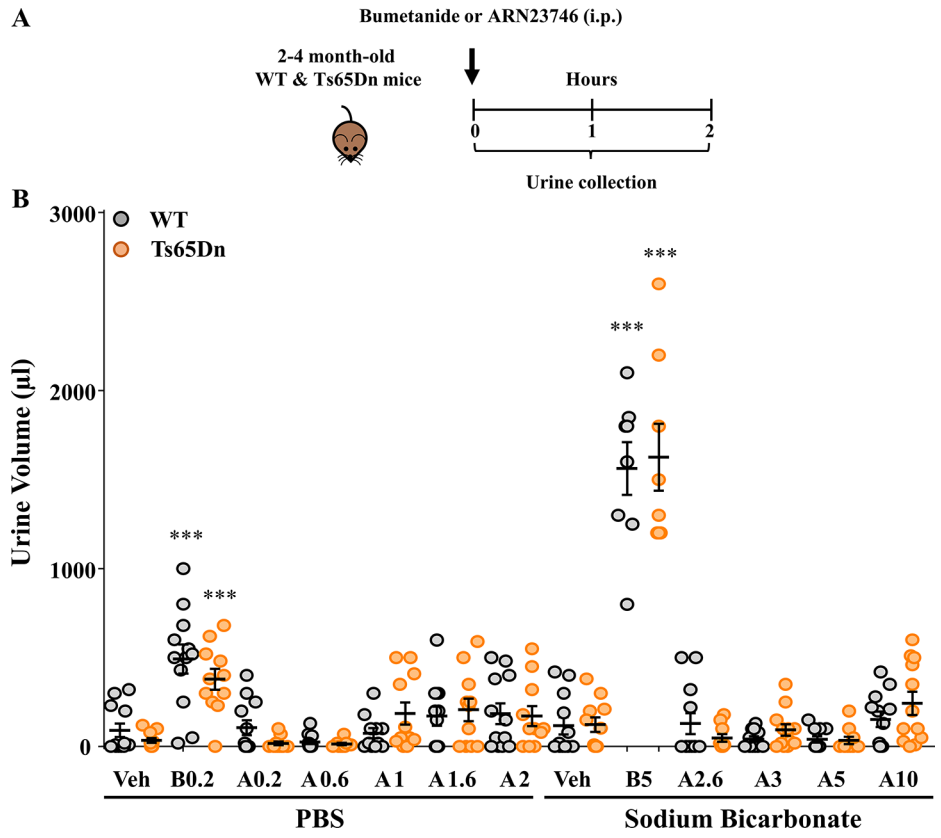

Figure 5. ARN23746 does not show a diuretic effect up to 10 mg kg^{-1}. (A) Schematic cartoon of the experimental protocol for the treatment of adult WT and Ts65Dn mice to assess the diuretic effect. (B) Quantification of the mean ± SEM and single animal cases of the urine volume collected for 120 min after mice were treated with the indicated drugs (Veh = Vehicle, B = Bumetanide, A = ARN23746) at the indicated increasing dosages (no. of single animals: PBS - WT Veh = 12, Ts65Dn Veh = 11, WT B0.2 = 12, Ts65Dn B0.2 = 11, WT A0.2 = 12, Ts65Dn A0.2 = 11, WT A0.6 = 12, Ts65Dn A0.6 = 10, WT A1 = 11, Ts65Dn A1 = 11, WT A1.6 = 12, Ts65Dn A1.6 = 11, WT A2 = 12, Ts65Dn A2 = 11; Sodium Bicarbonate - WT Veh = 12, Ts65Dn Veh = 11, WT B5 = 8, Ts65Dn B5 = 8, WT A2.6 = 10, Ts65Dn A2.6 = 11, WT A3 = 12, Ts65Dn A3 = 11, WT A5 = 11, Ts65Dn A5 = 10, WT A10 = 12, Ts65Dn A10 = 12; two-way ANOVA, $F_{\text{treatment }(5,117)} = 140.332$, $P < 0.001$, Tukey's *post hoc* test, ***$P < 0.001$). One outlier was excluded from the following groups: Ts65Dn Veh (PBS), Ts65Dn B0.2, Ts65Dn A0.2, WT A1, Ts65Dn A1, Ts65Dn A1.6, Ts65Dn A2, Ts65Dn Veh (Sodium Bicarbonate), WT A3; two outliers were excluded from the following groups: Ts65Dn A0.6, Ts65Dn A2.6 based on Grubbs's test. Two different vehicle solutions (PBS and Sodium Bicarbonate 1.4%) were used to facilitate the solubilization of ARN23746 at the different dosages. Higher concentrations (from 2.6 mg·kg^{-1}) were soluble only in a basic buffer.

IP: 18 629 h·ng/mL, AUC PO: 18 533 h·ng/mL; Figure 2A, C, D, F). After PO administration, the peak brain concentration was reached 15 min after administration in a concentration of 529 ng/g (Figure 2E, F). Interestingly, the PO mean brain−plasma ratio was 0.068, indicating an adequate brain penetration of the compound (Figure 2F).[10]

The oral route is preferred for drug administration, in particular in children, mainly due to its non-invasiveness and patient compliance.[11] In our previous work, ARN23746 rescued core brain-related symptoms of two different neurodevelopmental disorders upon IP administration (i.e., cognitive impairment in DS mice and social/repetitive behaviors in a mouse model of autism).[5] To develop further our lead candidate through clinical phases, specifically for such neurodevelopmental indications in children, we tested its ability to rescue cognitive impairments in DS mice (Ts65Dn Down syndrome mouse model) also using oral administration. In particular, we evaluated long-term hippocampus-dependent explicit memory and hyperactivity in adult male Ts65Dn and WT mice (post-natal day (P) 60−120), a widely used mouse model of DS. We administered ARN23746 at ≃2.5 mg·kg^{-1} in drinking water supplemented with 0.3% sucrose, or its vehicle (0.15% DMSO in drinking water supplemented with 0.3% sucrose), for 7−14 days to Ts65Dn and WT mice (Figure 3A). ARN23746 sub-chronic PO administration completely rescued the poor novel-discrimination ability of Ts65Dn mice,[12] which we assessed in the novel-object recognition (NOR) test (Figure 3B). ARN23746's effect in the NOR test was not due to biased object preference (Table S2). Moreover, ARN23746 rescued the hyperactivity of Ts65Dn mice, expressed as distance traveled and average walking speed during the open-field free exploration of a squared arena (Figure 3C). Investigation of ARN23746 efficacy in female Ts65Dn and WT mice will further validate the therapeutic potential of the compound.

Notably, all mice were healthy during the whole 2 weeks of continuous PO treatment with ARN23746, as evaluated by daily visual assessment and body weight measures (Figure 4A). Moreover, since treatment in new-born babies with a non-selective NKCC1 inhibitor (bumetanide) has been linked to hearing loss in a clinical study,[13] we also evaluated possible impairment in the auditory system upon ARN23746 administration. In particular, we assessed acoustic startle reactivity response by exposing mice sub-chronically PO treated with ARN23746 to a 90 dB sudden sound. In these experimental conditions, the hearing ability of WT and

https://doi.org/10.1021/acsptsci.2c00197
ACS Pharmacol. Transl. Sci. 2023, 6, 1−11

Ts65Dn mice after 2 weeks of continuous PO treatment with ARN23746 was perfectly retained, with no sign of auditory system damage (Figure 4B). A thorough investigation of hearing abilities in rodents and non-rodent species will further elucidate potential ototoxic effects at higher dosages. Importantly, we also assessed the diuretic effect of orally administered ARN23746, since bumetanide has strong diuretic effects and it is in fact FDA-approved for use as a potent diuretic in humans.[14] Toward this goal, we treated Ts65Dn mice and their WT littermates overnight with ARN23746 (0.015 mg·mL^{-1} of 10 mg·mL^{-1} stock solution in drinking water supplemented with 0.3% sucrose), bumetanide (0.015 mg·mL^{-1} of 10 mg·mL^{-1} stock solution in drinking water supplemented with 0.3% sucrose, as positive control), or vehicle (0.15% DMSO in drinking water supplemented with 0.3% sucrose) and assessed urine volume after overnight collection by metabolic cages (Figure 4C). Of note, the diuretic bumetanide induced more overnight water consumption in treated mice (7.5 ± 0.5 mL) compared to animals treated with ARN23746 (4.0 ± 0.2 mL) or vehicle (3.8 ± 0.2 mL). This leads to higher bumetanide calculated dosage per night (≃4 mg·kg^{-1}), compared to the calculated dosage of ARN23746 (≃2 mg·kg^{-1}). As expected, both WT and Ts65Dn bumetanide-treated mice showed an increased urine volume compared to vehicle-treated mice. Conversely, ARN23746 oral treatment had no significant diuretic effect in WT or Ts65Dn mice (Figure 4D).

Recently, a Phase III trial assessing the efficacy of bumetanide in autistic children was prematurely terminated due to the lack of efficacy (NCT03715153). The use of a low (sub-optimal) dosage of bumetanide (0.5 mg twice daily vs 2 mg twice daily assessed in a previous Phase II clinical trial[15]) to avoid excessive diuresis and severe side effects may be a possible factor contributing to this failure, which would be otherwise unexpected given the several successful Phase II clinical studies.[15−18] In this scenario, using a non-diuretic NKCC1 inhibitor such as ARN23746 would allow the administration of higher and optimally effective dosages, possibly granting success of future trials. In this specific case, a higher dosing of the drug—devoid of diuretic effects—could lead to better efficacy of the treatment because of higher NKCC1 inhibition. Moreover, the lack of diuretic effects would grant better treatment compliance, which would in turn reduce the dropout rate during the clinical trials and good toleration of the treatment in real-life scenarios. Finally, the absence of increased diuresis during the clinical study would allow to better maintain the double-blind scheme of the trial—which is a tricky aspect and potentially dangerous bias in trials involving diuretic drugs like bumetanide. Thus, to identify a possible therapeutic window, we assessed the diuretic effect of ARN23746 at increasing dosages of administration in WT and Ts65Dn mice. We measured the urine volume for 2 h following treatment with ARN23746 (0.2, 0.6, 1, 1.6, 2, 2.6, 3, 5, and 10 mg·kg^{-1}, IP) or bumetanide as positive control (0.2 and 5 mg·kg^{-1}, IP) (Figure 5A). WT and Ts65Dn mice treated with both bumetanide dosages showed a significantly increased urine volume compared to vehicle-treated mice. Conversely, ARN23746 treatment had no significant diuretic effect in WT or Ts65Dn mice at all the nine dosages administered (up to 10 mg·kg^{-1}; Figure 5B). This suggests that ARN23746 may be administered at least up to 50-fold higher than the effective dose (0.2 mg·kg^{-1}, IP),[5] without showing any sign of diuresis.

In this study, we performed an extensive preclinical characterization of ARN23746 both *in vitro* and *in vivo* to advance it to further preclinical and clinical studies. ARN23746 showed a promising overall profile in terms of potency, brain penetration, and metabolism. Moreover, ARN23746 was demonstrated to be suitable for oral treatment, showing efficacy in rescuing cognitive impairments in DS mice upon PO administration, without overt toxicity or diuretic effect. This is a crucial feature for the further clinical development of this lead compound, especially in pediatric populations with neurodevelopmental disorders. Finally, ARN23746 showed to be devoid of diuretic effect up to the 10 mg·kg^{-1} dosage, indicating a high therapeutic index. Overall, these data further indicate ARN23746 as a solid candidate for advanced preclinical development toward its evaluation in clinical studies. In particular, safety pharmacology and general toxicology studies will further evaluate the safety profile of ARN23746, including potential clinical signs due to the inhibition of NKCC1 in peripheral tissues[19] (e.g., lungs, intestine, salivary glands). ARN23746 will eventually represent a unique therapeutic option for the treatment of neurodevelopmental disorders characterized by impaired Cl^- balance.

EXPERIMENTAL PROCEDURES

HEK Cell Culture and Transfection. HEK293T cells were cultured and transfected as described in our previous works.[5,6] Briefly, cells were maintained in Dulbecco's Modified Eagle Medium (DMEM) supplemented with 10% fetal bovine serum, 1% L-glutamine, 100 U/mL penicillin, and 100 μg/mL streptomycin, at 37 °C in a 5% CO_2 humidified atmosphere. To perform Cl^--influx assay, 3 million HEK293T cells were plated in a 10 cm cell-culture dish and transfected with a transfection mixture comprising 5 mL of DMEM, 4 mL of Opti-MEM, 8 μg of mbYFPQS plasmid (Addgene #80742),[20] 8 μg of PRK-NKCC1 plasmid or empty PRK plasmid as mock control, and 32 μL of Lipofectamin 2000. After 4 h, the cells were collected and plated in 96-well black-walled, clear-bottomed plates at a density of 2.5 × 10^4. After 48 h, cells were used for the assay. All reagents were purchased from Life Technologies, unless otherwise specified.

Cl^--Influx Assay in HEK cells. The assay was performed as described in our previous works.[5,6] Briefly, transfected cells were treated with DMSO (as negative control) or with different concentrations (0.05−500 μM range) of ARN23746 in 200 μL/well of a Cl^--free hypotonic solution (67.5 mM Na^+ Gluconate, 2.5 mM K^+ Gluconate, 15 mM HEPES pH 7.4, 5 mM Glucose, 1 mM Na_2HPO_4, 1 mM NaH_2PO_4, 1 mM $MgSO_4$, 1 mM $CaSO_4$) and incubated for 30 min. Then, plates were loaded into a Tecan Spark multiplate reader equipped with an automatic liquid injector system, and the fluorescence of Cl^--sensitive mbYFPQS was measured (excitation 485 nm and emission 535 nm). For each well, fluorescence was recorded for 20 s of baseline and then for 60 s after application of a NaCl solution (74 mM final concentration in assay well). Florescence of mbYFPQS inversely correlates to the intracellular Cl^- concentration;[20] therefore, chloride influx into the cells causes a decrease of mbYFPQS fluorescence. For the data analysis, we normalized the fluorescence value for each time point to the average of the fluorescence value of the first 20 s of baseline ($\Delta F/F_0$), and we expressed the decrease in fluorescence upon NaCl application as the average of the last 10 s of normalized fluorescence values. Moreover, for each

https://doi.org/10.1021/acsptsci.2c00197
ACS Pharmacol. Transl. Sci. 2023, 6, 1−11

plate, to isolate the sole contribution of NKCC1 in Cl^- changes, we subtracted the value of the last 10 s of $\Delta F/F_0$ normalized values obtained from mock cells (either control or treated) from the respective $\Delta F/F_0$ values obtained from the NKCC1-transfected cells. We then calculated the percentage of the fluorescence decrease normalized to the control DMSO, and consequently the percentage of inhibition (100 − % of fluorescence decrease). Finally, we fitted the dataset on NKCC1 inhibition by ARN23746 at different concentrations (0.05−500 μM range) expressed on a logarithmic scale with a non-linear curve to extrapolate the corresponding IC_{50}.

Neuron Cultures. To perform the Ca^{2+}-influx assay, primary neuronal cultures of dissociated hippocampal neurons were prepared from E18 C57BL/6J mice (Charles River), as described in our previous works,[5,6] and plated in 96-well black-walled, clear-bottomed plates coated with poly-L-lysine (Sigma; 0.1 mg/mL in 100 mM borate buffer, pH 8.5) at a density of 30 000 cells per well. Neurons were maintained in Neurobasal medium supplemented with 2% B-27, 0.5 mM glutamine, 50 U/mL of penicillin, and 50 μg/mL of streptomycin (all from Gibco) and incubated at 37 °C and 5% CO_2 until DIV 3 for the Ca^{2+}-influx assay. To perform the Western blot experiment, 500 000 hippocampal neurons (obtained with the same preparation method described above) were plated on 6-well plates coated with poly-L-lysine, and maintained in culture until DIV 3 or DIV 21.

Ca^{2+}-Influx Assay in Neuronal Cultures. The assay was performed as described in our previous works.[5,6] Briefly, 3 DIVs neurons were loaded with 2.5 μM of the calcium-sensitive dye Fluo4-AM (Invitrogen) in extracellular solution (145 mM NaCl, 5 mM KCl, 10 mM HEPES, 5.55 mM Glucose, 1 mM $MgCl_2$, 2 mM $CaCl_2$, pH 7.4) for 15 min. Then, cells were washed twice with extracellular solutions and treated with DMSO (as negative control), and with different concentrations (0.01−500 μM range) of ARN23746, in extracellular solution for 15 min. Plates were then loaded into a Tecan Spark multiplate reader equipped with an automatic liquid injector system and Fluo4 fluorescence was measured (excitation 485 nm and emission 535 nm). For each well, fluorescence was recorded for 20 s of baseline and for 20 s after delivery of GABA (10 μM final concentration in wells), followed by 20 s upon application of a depolarizing KCl stimulus (90 mM final concentration in wells), to evaluate neuronal viability. For the analysis, we normalized the fluorescence value for each time point to the average of the fluorescence value for the first 20 s of baseline ($\Delta F/F_0$). Then, we extrapolated the maximum peak increase in $\Delta F/F_0$ fluorescence upon GABA application and we normalized it over the maximum peak increase in $\Delta F/F_0$ fluorescence upon KCl application. We then calculated the percentage of the fluorescence increase normalized to the control DMSO, and consequently the percentage of inhibition (100 − % of fluorescence increase). Finally, we fitted the dataset on inhibition of Ca^{2+} responses by ARN23746 at different concentrations (0.01−500 μM range) expressed on a logarithmic scale with a non-linear curve to extrapolate the corresponding IC_{50}.

Biochemistry. Cell lysis and Western blot were performed as described in our previous work.[5] Briefly, cells were lysated in RIPA buffer (1% NP40, 0.5% Deoxycholic acid, 0.1% SDS, 150 mM NaCl, 1 mM EDTA, 50 mM Tris, pH 7.4) supplemented with 1% (v/v) protease and phosphatase inhibitor cocktails (Sigma) for 30 min in ice. Then, the samples were clarified by centrifugation (20000*g* for 20 min at 4 °C). The protein concentration was determined with a BCA kit (Pierce). To perform Western blot, samples were diluted in lithium-dodecyl-sulfate (LDS) buffer (ThermoFisher Scientific) supplemented with 50 mM DTT and warmed at 40 °C for 5 min.[21] 20 μg samples of protein were loaded on the 4−12% Bis-Tris NuPAGE precast gels (Invitrogen), and electrophoresis was performed with MOPS buffer (Life Technologies). Next, gels were transferred overnight at 4 °C onto nitrocellulose membranes (GE Healthcare) with Tris-Glycine transfer buffer (25 mM Tris-base, 192 mM glycine, 20% Methanol). Equal amounts of protein loading was verified by staining with 0.1% Ponceau. Membrane blocking was performed in 5% milk in Tris-buffered saline (10 mM Tris, 150 mM NaCl, pH 8.0) plus 0.1% Tween-20 for 1 h. Then, membranes were incubated overnight at 4 °C with primary antibodies, rabbit anti-actin (Sigma, catalog no. A2066; 1:10 000) and mouse anti-NKCC1 (clone T4c, Developmental Studies Hybridoma Bank; 1:4000). Next, membranes were washed, incubated for 2 h at room temperature with HRP-conjugated goat secondary antibodies (ThermoFisher Scientific; 1:10 000), and developed with SuperSignal West Pico chemiluminescent substrate (ThermoFisher Scientific). The chemiluminescent signals were captured by the LAS 4000 Mini imaging system (GE Healthcare).

Pharmacokinetic Analysis. An external contractor performed the study. Additional information on the study conditions can be obtained from the contractor's website.[22] ARN23746 was administered IP or PO at 10 mg/kg in sodium bicarbonate buffer 1.4%, pH 8.3, with 2% DMSO to adult C57BL/6N mice (Charles River, Italy). Blood was collected by cardiac puncture at 0.083, 0.25, 0.5, 1, 2, 4, 8, and 24 h. Blood aliquots were collected in tubes coated with lithium heparin, mixed gently, then kept on ice and centrifuged at 2500*g* for 10 min at 4 °C, within 0.5 h of collection. The plasma was then harvested and stored frozen at 4 °C until further analysis. After the blood collection, mice were decapitated and the whole brains were quickly removed and stored at 4 °C until further analysis. Samples were then processed using a method based on protein precipitation with acetonitrile followed by UPLC/MS-MS analysis. The fundamental pharmacokinetic parameters after dosing (plasma and brain concentration, AUC_{last}, AUC_{inf}, $T_{1/2}$, Cl, V_z, V_{ss}, T_{max}, and C_{max}) were obtained from the non-compartmental analysis (NCA) of the plasma/brain data using Phoenix WinNonlin.

Animals. All animal procedures were approved by IIT licensing in compliance with the Italian Ministry of Health (D.Lgs 26/2014) and EU guidelines (Directive 2010/63/EU). A veterinarian was responsible of the maintenance of the health and comfort of the animals. Mice were housed in filtered cages in a temperature-controlled room with a 12:12 h dark/light cycle and with *ad libitum* access to water and food. All efforts were made to minimize animal suffering and use the lowest possible number of animals required to produce statistically relevant results, according to the "3Rs concept". Ts65Dn mice used in this study derived from internal colony, where we maintained animals in their original genetic background[12] by crossing (more than 40 times) Ts65Dn female to C57BL/6JEi × C3SnHeSnJ (B6EiC3) F1 males (Jackson Laboratories). Ts65Dn mice were genotyped using the PCR protocol previously described.[23] Male offspring aged between 2 and 4 months were used for experiments. For behavioral and diuresis experiments upon *per os* (PO) administration, Ts65Dn mice

https://doi.org/10.1021/acsptsci.2c00197
ACS Pharmacol. Transl. Sci. 2023, 6, 1−11

with their respective controls were randomly assigned to vehicle group (0.15% DMSO in drinking water supplemented with 0.3% sucrose), bumetanide (Sigma, 4 mg·kg^{-1} in drinking water supplemented with 0.3% sucrose), or ARN23746 (2−2.5 mg·kg^{-1} in drinking water supplemented with 0.3% sucrose), and continuously treated for 7−14 days (drinking water was changed every 3−4 days). For experiments assessing the diuretic effect of ARN23746 at increasing dosages of administration, Ts65Dn mice with their respective controls were randomly assigned to vehicle group (0.2% DMSO in PBS or in 1.4% sodium bicarbonate buffer), bumetanide (Sigma, 0.2 mg·kg^{-1} in PBS or 5 mg·kg^{-1} in 1.4% sodium bicarbonate buffer), or ARN23746 (0.2, 0.6, 1, 1.6, or 2 mg·kg^{-1} in PBS or 2.6, 3, 5, or 10 mg·kg^{-1} in 1.4% sodium bicarbonate buffer) and treated for 1 day by intraperitoneal injection (IP).

Compound Preparation for *In Vivo* Experiments. For the *in vivo* experiments upon PO administration, bumetanide and ARN23746 were dissolved in DMSO in a stock solution of 10 mg/mL. The stock solution was dissolved in drinking water supplemented with 0.3% sucrose at a concentration of 0.015 mg·mL^{-1}. The vehicle group received 0.15% DMSO in drinking water supplemented with 0.3% sucrose. For behavioral experiments, considering the volume of water drunk by each mouse per day (vehicle: 4.7 ± 0.3 mL; ARN23746: 5.0 ± 0.2 mL), we calculated the range of ARN23746 assumption (2.5 ± 0.1 mg·kg^{-1}). For diuresis experiments upon PO administration, considering the volume of water drunk by each mouse during the 14 h overnight, (vehicle: 3.8 ± 0.2 mL; bumetanide: 7.5 ± 0.5 mL; ARN23746: 4.0 ± 0.2 mL), we calculated the range of drug assumption (bumetanide: 4 ± 0.3 mg·kg^{-1}; ARN23746: 2 ± 0.1 mg·kg^{-1}). For diuresis experiments upon IP administration, bumetanide and ARN23746 were dissolved in DMSO in stock solutions at different concentrations that we dissolved in PBS or 1.4% sodium bicarbonate buffer to have a final concentration of DMSO equal to 2% in the injected volume (10 μL·g^{-1}).

Behavioral Testing. Ts65Dn male mice (2−4 months old) were tested after 1 week of continuous treatment with vehicle or ARN23746 (2.5 mg·kg^{-1} in drinking water supplemented with 0.3% sucrose). The battery of tests was performed over a total period of ∼7 days (with the following order: Open Field, NOR). The tests were video-recorded and then scored manually by an operator blind to the experimental groups. After each trial, all the apparatuses and objects were cleaned with 70% ethanol. *Open Field Test.* The test evaluates the locomotor activity of mice, measured as total distance traveled and average walking speed during the free exploration on day 1 of the NOR test. The task was performed as described in our previous work.[6] Briefly, mice were placed in gray acrylic arenas (44 × 44 cm), evenly illuminated by overhead red lighting (12−14 lx), and were allowed to freely explore them for 15 min. Any-Maze software (Stoelting Co.) was used to track the animals and to extrapolate the locomotor activity parameters *Novel Object Recognition Test (NOR).* The test assesses long-term object recognition memory by measuring the mice's ability to recognize a new object in comparison to familiar objects. The test was performed as described in our previous works.[5,6] Briefly, mice were placed in gray acrylic arenas (44 × 44 cm), evenly illuminated by overhead red lighting (12−14 lx). On day 1 (habituation phase), mice were allowed to freely explore the arena for 15 min. On day 2 (acquisition phase), three different objects (different in color, size, shape, material) were placed in the arenas, and mice were free to explore them for 15 min. After 24 h (test phase), one object from the acquisition phase was replaced with a new one, and the mice were tested for 15 min for their ability to recognize the novel object. We scored the time spent exploring each object (expressed as a percentage of the total exploration time) by measuring the seconds during which mice showed investigative behavior (i.e., head orientation, sniffing occurring within <1.0 cm) or clear contact between the object and the nose. The discrimination index was calculated with the following formula: discrimination index = (novel object exploration time/total exploration time × 100) − (familiar object exploration time/total exploration time × 100). As control, we monitored object preference during the acquisition phase, and exploration time in the acquisition phase and trial phase. Of note, although there was a genotype preference (WT vs Ts65Dn) of the object C within the vehicle-treated animals (Table S2), the objects were randomly replaced with new ones for the test phase, thus not affecting the final result. In the NOR test, we excluded two animals showing very low explorative behavior (<20 s of direct object exploration during 15 min acquisition and/or test phases). This exclusion criterion was independent of genotype or treatment and applied before blind code was broken.

Acoustic Startle Response. The acoustic startle response test evaluates the reactivity to a sudden and intense acoustic stimulus.[24] At the end of the behavioral tests, each mouse was placed in a plastic open cage, and a sudden sound (20 kHz, 90 dB at 30 cm distance) was produced by a specific device. The response to the acoustic stimulus was measured as a rapid contraction of facial and skeletal muscle with the following score scale: 0 = no response, 1 = mild response, 2 = complete response. Each mouse performed three trials (three acoustic stimuli of the same intensity every 5 s intervals) and the scores were averaged.

Diuresis Analysis. Diuresis analysis was performed as described in our previous works.[5,6] Briefly, mice were placed in metabolic cages (one animal per cage, Tecniplast, 3600M021) equipped with a grid over a funnel and a plastic cone for the separate collection of urine and feces. To assess ARN23746 diuretic effect upon PO administration, animals were placed overnight inside the metabolic cages where food and water supplemented with 0.3% sucrose, in which we dissolved the different compounds (0.15% DMSO, bumetanide 0.015 mg·mL^{-1}; ARN23746 0.015 mg·mL^{-1}), were available *ad libitum*. After 14 h, mice were returned to their home cages, and the urine volume was measured. To assess ARN23746 diuretic effect upon IP administration, immediately after IP injection with vehicle (2% DMSO in PBS or 1.4% sodium bicarbonate buffer), bumetanide (Sigma, 0.2 mg·kg^{-1} in PBS or 5 mg·kg^{-1} in 1.4% sodium bicarbonate buffer), or ARN23746 (0.2, 0.6, 1, 1.6, and 2 mg·kg^{-1} in PBS or 2.6, 3, 5, and 10 mg·kg^{-1} in 1.4% sodium bicarbonate buffer), animals were placed inside the metabolic cages where food and water were available *ad libitum*. After 2 h, mice were returned to their home cages, and the urine volume was measured.

Statistical Analysis. The results are presented as the means ± SEM. The statistical analysis was performed using SigmaPlot 13.0 (Systat) software. Where appropriate, the statistical significance was assessed using the parametric test two-way ANOVA followed by all-pairwise Tukey *post hoc* test. Where normal distribution or equal variance assumptions were not valid, statistical significance was evaluated using two-way

https://doi.org/10.1021/acsptsci.2c00197
ACS Pharmacol. Transl. Sci. 2023, 6, 1−11

ANOVA on ranks followed by all pairwise Dunn's *post hoc* test. *P* values <0.05 were considered significant. Outliers were excluded only from the final pool of data by a Grubbs's test (GraphPad, alpha = 0.05) run iteratively until no outliers were found.

■ ASSOCIATED CONTENT

Supporting Information

The Supporting Information is available free of charge at https://pubs.acs.org/doi/10.1021/acsptsci.2c00197.

Procedures for *in vitro* permeability determination and P-gp interaction in MADCKII MDR1 cells, *in vitro* permeability determination and BCRP interaction in Caco-2 cells, *in vitro* mouse microsomes stability, *in vitro* mouse, rat, and human liver hepatocytes stability and metabolites identification, Figure S1 (uncropped Western blot membranes related to the Figure 1A), Table S1 (*in vitro* permeability assessment and metabolism analysis of ARN23746), and Table S2 (control parameters in the NOR tasks of WT and Ts65Dn mice) (PDF)

■ AUTHOR INFORMATION

Corresponding Authors

Annalisa Savardi − *IAMA Therapeutics, 16128 Genoa, Italy;* orcid.org/0000-0002-1171-8048; Email: marco.borgogno@iamatherapeutics.com

Marco Borgogno − *IAMA Therapeutics, 16128 Genoa, Italy;* orcid.org/0000-0003-0921-7516; Email: annalisa.savardi@iamatherapeutics.com

Authors

Andrea Patricelli Malizia − *IAMA Therapeutics, 16128 Genoa, Italy*

Marco De Vivo − *IAMA Therapeutics, 16128 Genoa, Italy; Molecular Modeling & Drug Discovery Laboratory, Istituto Italiano di Tecnologia, 16163 Genoa, Italy;* orcid.org/0000-0003-4022-5661

Laura Cancedda − *IAMA Therapeutics, 16128 Genoa, Italy; Brain Development & Disease Laboratory, Istituto Italiano di Tecnologia, 16163 Genoa, Italy*

Complete contact information is available at: https://pubs.acs.org/10.1021/acsptsci.2c00197

Author Contributions

A.S. designed and performed *in vitro* assays, Western blot, behavioral experiments, and diuresis experiment and analyzed data. M.B. designed and synthesized the compounds. A.S., M.B., M.D.V., and L.C. designed the experiments and analyzed the data. All authors contributed to the writing and critical assessment of the manuscript and its content.

Funding

Telethon grant TCP15021 to L.C. This project received partial funding from the European Research Council (ERC) under the European Union's Horizon 2020 research and innovation program (grant agreement no. 725563 to L.C.).

Notes

The authors declare the following competing financial interest(s): L.C. is named as co-inventor on the following granted patents: US 9,822,368, EP 3083959, and JP 6490077; A.S., M.B., M.D.V., and L.C. are named as co-inventors on patent application IT 102019000004929. A.S., M.B., and A.P.M. are employees of IAMA Therapeutics, while L.C. and M.D.V. are scientific founders and act as consultants of IAMA Therapeutics.

■ ACKNOWLEDGMENTS

We thank Marina Nanni (IIT) and the staff of the IIT animal facility for the technical support.

■ ABBREVIATIONS USED

ARN23746, 3-(*N*,*N*-dimethylsulfamoyl)-4-((8,8,8-trifluorooctyl)amino)-benzoic acid; Bume, Bumetanide; BBB, blood−brain barrier; BCRP, Breast Cancer Resistance Protein; $[Cl^-]_i$, intracellular chloride concentration; CNS, central nervous system; DMSO, dimethyl sulfoxide; DS, Down syndrome; IP, intraperitoneal; HEK293T, human embryonic kidney 293 cells; MDCKII-MDR1, Madin−Darby Canine Kidney−Multi-Drug resistance 1; MetID, metabolites identification; NHP, non-human primates; PO, *per os*; NOR, novel object recognition; P-gp, P-glycoprotein; Ts65Dn, Down syndrome mouse model; WT, wild-type.

■ REFERENCES

(1) Deidda, G.; Bozarth, I. F.; Cancedda, L. Modulation of GABAergic transmission in development and neurodevelopmental disorders: investigating physiology and pathology to gain therapeutic perspectives. *Frontiers in cellular neuroscience* **2014**, *8*, 119.

(2) Ben-Ari, Y. NKCC1 Chloride Importer Antagonists Attenuate Many Neurological and Psychiatric Disorders. *Trends in neurosciences* **2017**, *40* (9), 536−554.

(3) Contestabile, A.; Magara, S.; Cancedda, L. The GABAergic Hypothesis for Cognitive Disabilities in Down Syndrome. *Frontiers in cellular neuroscience* **2017**, *11*, 54.

(4) Schulte, J. T.; Wierenga, C. J.; Bruining, H. Chloride transporters and GABA polarity in developmental, neurological and psychiatric conditions. *Neuroscience and biobehavioral reviews* **2018**, *90*, 260−271.

(5) Savardi, A.; Borgogno, M.; Narducci, R.; La Sala, G.; Ortega, J. A.; Summa, M.; Armirotti, A.; Bertorelli, R.; Contestabile, A.; De Vivo, M.; et al. Discovery of a Small Molecule Drug Candidate for Selective NKCC1 Inhibition in Brain Disorders. *Chem* **2020**, *6* (8), 2073−2096.

(6) Borgogno, M.; Savardi, A.; Manigrasso, J.; Turci, A.; Portioli, C.; Ottonello, G.; Bertozzi, S. M.; Armirotti, A.; Contestabile, A.; Cancedda, L.; et al. Design, Synthesis, In Vitro and In Vivo Characterization of Selective NKCC1 Inhibitors for the Treatment of Core Symptoms in Down Syndrome. *J. Med. Chem* **2021**, *64* (14), 10203−10229.

(7) Watanabe, M.; Fukuda, A. Development and regulation of chloride homeostasis in the central nervous system. *Frontiers in cellular neuroscience* **2015**, *9*, 371.

(8) Xiong, B.; Wang, Y.; Chen, Y.; Xing, S.; Liao, Q.; Chen, Y.; Li, Q.; Li, W.; Sun, H. Strategies for Structural Modification of Small Molecules to Improve Blood-Brain Barrier Penetration: A Recent Perspective. *J. Med. Chem.* **2021**, *64* (18), 13152−13173.

(9) Okour, M.; Brundage, R. C. Modeling Enterohepatic Circulation. *Current Pharmacology Reports* **2017**, *3*, 301−313.

(10) Bakthavatchalam, R.; Kimball, S. D. Defining Neuropharmacokinetic Parameters in CNS Drug Discovery to Determine Cross-species Pharmacologic Exposure-Response Relationships. In *Annual Reports in Medicinal Chemistry*, Vol. *45*; Macor, J., Ed.; Elsevier, 2010; pp 55−70.

(11) Alqahtani, M. S.; Kazi, M.; Alsenaidy, M. A.; Ahmad, M. Z. Advances in Oral Drug Delivery. *Frontiers in pharmacology* **2021**, *12*, 618411.

(12) Reeves, R. H.; Irving, N. G.; Moran, T. H.; Wohn, A.; Kitt, C.; Sisodia, S. S.; Schmidt, C.; Bronson, R. T.; Davisson, M. T. A mouse

model for Down syndrome exhibits learning and behaviour deficits. *Nat. Genet.* **1995**, *11* (2), 177−184.
(13) Ben-Ari, Y.; Damier, P.; Lemonnier, E. Failure of the Nemo Trial: Bumetanide Is a Promising Agent to Treat Many Brain Disorders but Not Newborn Seizures. *Frontiers in cellular neuroscience* **2016**, *10*, 90.
(14) Sidhu, G.; Puckett, Y. Bumetanide. *StatPearls*, March 15, 2022. https://www.ncbi.nlm.nih.gov/books/NBK559181/
(15) Lemonnier, E.; Villeneuve, N.; Sonie, S.; Serret, S.; Rosier, A.; Roue, M.; Brosset, P.; Viellard, M.; Bernoux, D.; Rondeau, S.; et al. Effects of bumetanide on neurobehavioral function in children and adolescents with autism spectrum disorders. *Transl. Psychiatry* **2017**, *7* (3), No. e1056.
(16) Lemonnier, E.; Degrez, C.; Phelep, M.; Tyzio, R.; Josse, F.; Grandgeorge, M.; Hadjikhani, N.; Ben-Ari, Y. A randomised controlled trial of bumetanide in the treatment of autism in children. *Transl. Psychiatry* **2012**, *2*, No. e202.
(17) Sprengers, J. J.; van Andel, D. M.; Zuithoff, N. P.; Keijzer-Veen, M. G.; Schulp, A. J.; Scheepers, F. E.; Lilien, M. R.; Oranje, B.; Bruining, H. Bumetanide for Core Symptoms of Autism Spectrum Disorder (BAMBI): A Single Center, Double-Blinded, Participant-Randomized, Placebo-Controlled, Phase Two, Superiority Trial. *Journal of the American Academy of Child and Adolescent Psychiatry* **2021**, *60*, 865.
(18) Du, L.; Shan, L.; Wang, B.; Li, H.; Xu, Z.; Staal, W. G.; Jia, F. A Pilot Study on the Combination of Applied Behavior Analysis and Bumetanide Treatment for Children with Autism. *Journal of child and adolescent psychopharmacology* **2015**, *25* (7), 585−588.
(19) Koumangoye, R.; Bastarache, L.; Delpire, E. NKCC1: Newly Found as a Human Disease-Causing Ion Transporter. *Function (Oxf)* **2020**, *2* (1), zqaa028.
(20) Watts, S. D.; Suchland, K. L.; Amara, S. G.; Ingram, S. L. A sensitive membrane-targeted biosensor for monitoring changes in intracellular chloride in neuronal processes. *PLoS One* **2012**, *7* (4), No. e35373.
(21) Deidda, G.; Parrini, M.; Naskar, S.; Bozarth, I. F.; Contestabile, A.; Cancedda, L. Reversing excitatory GABAAR signaling restores synaptic plasticity and memory in a mouse model of Down syndrome. *Nature medicine* **2015**, *21* (4), 318−326.
(22) https://www.evotec.com/en/execute/drug-discovery-services
(23) Reinholdt, L. G.; Ding, Y.; Gilbert, G. J.; Czechanski, A.; Solzak, J. P.; Roper, R. J.; Johnson, M. T.; Donahue, L. R.; Lutz, C.; Davisson, M. T. Molecular characterization of the translocation breakpoints in the Down syndrome mouse model Ts65Dn. *Mamm. Genome* **2011**, *22* (11−12), 685−691.
(24) Koch, M. The neurobiology of startle. *Progress in neurobiology* **1999**, *59* (2), 107−128.

https://doi.org/10.1021/acsptsci.2c00197
ACS Pharmacol. Transl. Sci. 2023, 6, 1−11